Preparation of transparent alumina thin films deposited by RF magnetron sputtering

Busarin NOIKAEW[1], Laksana WANGMOOKLANG[1], Saisamorn NIYOMSOAN[2,*], and Siriporn LARPKIATTAWORN[1]

[1] *Expert Centre of Innovative Materials, Thailand Institute of Scientific and Technological Research, Pathum Thani, 12120, Thailand*
[2] *Integrated & Innovative Jewelry Materials Research Unit, Faculty of Gems, Burapha University, Chanthaburi, 22170, Thailand*

*Corresponding author e-mail: saisamor@go.buu.ac.th

Abstract

Alumina (Al_2O_3) thin films were prepared by RF magnetron sputtering technique using Al_2O_3 ceramic target. Effects of sputtering powers and oxygen gas mixtures were investigated and the optimized coating condition was applied on semi-precious gemstones. RF sputtering powers were varied to optimize the transparency of the films. Besides, the oxygen gas mixtures were also studied at the optimized sputtering power with a constant sputtering pressure. Optical and physical properties of the thin films were investigated using UV-Vis Spectrophotometer, FESEM, XRF, GIXRD, XRR including a microscratch tester. The Al_2O_3 films were highly transparent in the visible region in form of an amorphous phase with granular structure of the surface morphology. Thickness of the films decreased significantly with an introduction of the oxygen gas in the sputtering process but slowly decreased with further addition of the oxygen gas. Density of the film changed linearly with the variation of the oxygen gas mixtures. The semi-precious gemstones gained higher scratch resistance after the Al_2O_3 thin films coating. To enhance the scratch resistance and maintain the aesthetic appearance of the semi-precious gemstones, the most optimum deposition condition for the Al_2O_3 thin film coating was determined for the RF magnetron sputtering technique at room temperature.

1. Introduction

Thin layer composite coatings are widely used as protective materials for surface modification against oxidation, wear and corrosion. In addition, cutting and forming tools in manufacture are extensively applied with the hard coating for improving heat reduction, cutting efficiency, cost reduction and energy saving [1,2]. Regularly, many composite coatings include metal oxides, carbides as well as nitrides such as Cr_2O_3, Al_2O_3, TiO_2, CeO_2, SiC, TiN, CrN and ZrN due to their desirable mechanical, tribological, chemical and optical properties [3]. Among these protective materials, aluminum oxide (Al_2O_3) or alumina is a highly insulating material with wide band gap (8.2 eV), low refractive index (1.65), high mechanical resistance, high hardness and good adhesion on various surfaces [4,5]. The alumina thin film has a broad range of applications on microelectronic, nanoelectronic and optoelectronic devices as antireflection layers, anticorrosive coatings, optical protective coatings and gas diffusion barriers [6-8]. Various deposition techniques have been applied for thin film fabrication including DC and RF magnetron sputtering [9-11], atomic layer deposition [12,13], spray pyrolysis [14,15] and chemical vapor deposition processes [16,17]. For enhancing the film uniformity and adhesion on a substrate, the magnetron sputtering is the most favorable technique for many types of coating materials such as oxides, nitrides, carbides, fluorides and arsenides [9-11].

In gems industry, surface coating technology has been applied mainly to improve colorless gemstones to many variety of colors such as diamond, topaz, cubic zirconia, including corals and pearls with both CVD and PVD techniques [18-23]. Apart for coloration, the coating may also act as a protective layer. Several companies offer DLC coating for surface durability on a variety of gemstone including emerald, apatite, peridot and aquamarine [21]. With the excellent properties, especially high hardness, high transparency and good adhesion, the Al_2O_3 thin films coating as also been developed as a protective layer for semi-precious gemstones by ALD process. The film can improve the mechanical resistance of the gemstones without changing their aesthetic appearance. [24-26]. Normally, amorphous phase of Al_2O_3 is dominated below 400°C, γ-Al_2O_3 phase and then α-Al_2O_3 phase are formed at higher temperatures, consecutively [27].

Many research works have developed the Al_2O_3 thin film coating for coating many types of materials using the magnetron sputtering. To create thin film uniformity and good adhesion of the Al_2O_3 thin films, the RF magnetron sputtering has been chosen over the DC magnetron sputtering for a requirement of an insulating Al_2O_3 ceramic target. Effects of several coating parameters has been studied to optimized the coating conditions [28-32].

With the main advantage of RF magnetron sputtering, the present study applied the RF magnetron sputtering process to prepare the Al_2O_3 thin films at room temperature to generate a protective coating for semi-precious gemstones. The different RF sputtering powers and oxygen gas mixtures were investigated for observing the highly optical transmission in visible region. Furthermore, surface morphology,

chemical composition, structure and thickness of the Al_2O_3 thin film were also studied including scratch resistance. The optimal coating condition of the Al_2O_3 thin films was applied for the semi-precious gemstones to improve the scratch resistance.

2. Experimental procedure

2.1 Thin film fabrication

The aluminum oxide (Al_2O_3) thin films were prepared by RF (13.56 MHz) magnetron sputtering technique using a commercial smart PVD and implantation system from Plasma Technology Ltd. (PVDI). A 99.99% Al_2O_3 ceramic target, which was 50.8 mm in diameter and 6 mm in thickness, was bonded with copper-backing plate for heat conduction and reducing a risk of crack on the target. Substrates were clear microscope glass slides (a commercial soda-lime-silica glass), stainless steel plates, silicon wafers and semi-precious gemstones (peridot and aquamarine). These substrates were cleaned sequentially in a 15 min ultrasonic bath of acetone, methanol and deionized water prior to deposition. The target-substrate separation was set at 10 cm and the base pressure in the chamber was approximately 2.0×10^{-4} Pa. In the deposition process, the Al_2O_3 target was bombarded with positive ions of argon gas. The sputtered plasma was generated and traveled to the substrate [33]. Schematic diagram of the RF sputtering technique is illustrated in Figure 1. The deposition process was performed at room temperature with a substrate rotation at a rate of 10 rpm. In the present study, effects of the deposition parameters were focused on the sputtering powers and the oxygen gas mixtures. Firstly, without oxygen gas mixture, the Al_2O_3 thin films were continuously deposited on the glass substrates for 30 min with the RF sputtering powers ranging from 30 W to 70 W to maximize transparency of the film. Consequently, the optimum sputtering power was further applied to the Al_2O_3 thin film deposition with different oxygen gas mixtures. The percentage by volume (vol%) of oxygen gas with respect to that of argon gas was varied from 0 vol% to

6 vol%. Total pressure of the gas mixtures remained constant at 6.0×10^{-1} Pa with the argon gas flow rate of 12 sccm. The deposition process with different oxygen gas mixtures was operated at room temperature for 300 min of deposition time with 10 min pauses at every 30 min. The deposition interval for this experiment was to reduce the accumulated heat at the Al_2O_3 ceramic target.

The physical properties of the deposited Al_2O_3 thin films were investigated to tune the RF sputtering powers and oxygen gas mixtures towards the optimum properties of the Al_2O_3 film. Accordingly, the semi-precious gemstone substrates including peridot and aquamarine were coated with the Al_2O_3 thin film by the sputtering process at the optimized deposition parameter. The physical properties of the gemstones deposited with the Al_2O_3 thin films were also investigated.

2.2 Thin film characterization

Optical properties of the transparent Al_2O_3 thin films deposited on glass substrates were analyzed by UV-Vis Spectrophotometer (UV-1700, SHIMADZU). Surface morphology of the Al_2O_3 thin films deposited on silicon wafers were observed by Field Emission Scanning Electron Microscope operated at 5 kV (FESEM, JEOL JSM-6340F). Besides, the composition ratios of the Al_2O_3 thin films deposited on stainless steel substrates were analyzed by X-ray Fluorescence (XRF, Bruker S8 Tiger). The structures of the Al_2O_3 thin films deposited on the glass substrate were characterized by grazing incidence X-ray diffraction (GIXRD, Rigaku SmartLab) at an incident angle of 1°. Thicknesses of the Al_2O_3 thin films deposited on silicon wafers were characterized by X-ray Reflectivity (XRR, Rigaku SmartLab). Nevertheless, coating adhesion of the Al_2O_3 films was investigated using Microscratch Tester with Rockwell diamond stylus indenter (MST^3, Anton Paar).

3. Results and discussion

3.1 Optical transmission

Optical transmission of the as-deposited Al_2O_3 thin films grown on the glass substrates were measured by UV-Vis Spectrophotometer as a function of wavelengths ranging from 300 nm to 1100 nm with respect to a bare glass substrate. By changing the RF powers from 30 W to 70 W, the Al_2O_3 obtained 70% to 90% transmission with a sharp absorption edge around 300 nm to 320 nm (Figure 2). The transmission of the films significantly increased as the sputtering power increased to 50 W, and it subsequently decreased with further increase of the sputtering power.

In accordance with the present study, the high optical transmission of the Al_2O_3 thin films deposited at room temperature was also observed in the research of García-Valenzuela [9] and Singh [28] where the sputtering was performed above 150 W at room temperature. The correlation showed that the Al_2O_3 thin film was highly transparent in nature. The higher RF power in the sputtering process induces the bombarding argon ions with higher kinetic energy, which increases the sputtering yield. [9,28]
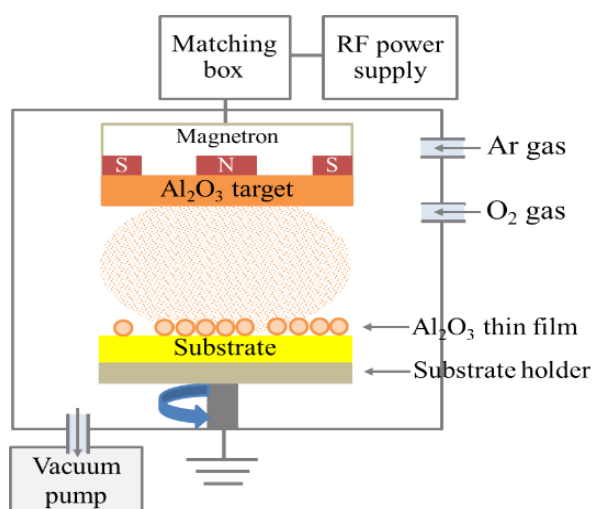

Figure 1. Schematic diagram of RF magnetron sputtering system for the Al_2O_3 thin film.
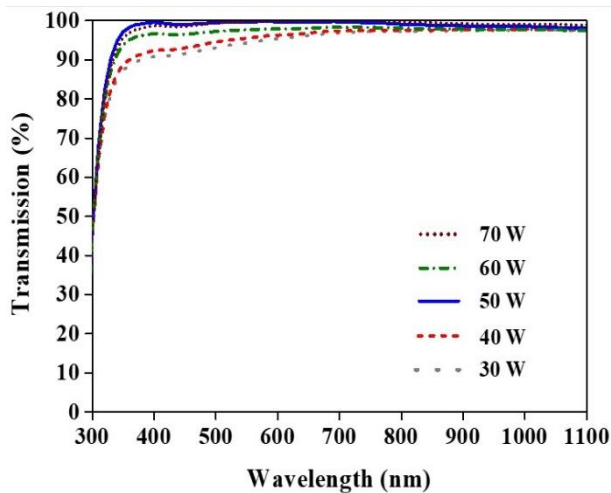
Figure 2. Influence of sputtering powers on optical transmission of the Al_2O_3 thin films.

Increasing the RF power resulted in a higher deposition rate and altered the optical properties of the films as it has been reported in literatures [9,34-38]. The optical transmission was influenced both by the roughness and thickness of the films. Several groups demonstrated that the optical transmission of the films decreased with higher roughness and thickness [9,34,35,38] due to high energy of sputtering particles as the RF power increased [32,39].

Effects of the oxygen gas mixtures on the optical transmission of the Al_2O_3 thin films deposited at 50 W sputtering power were shown in Figure 3. All the films exhibited excellent transmission (around 95% to 99%) in the visible region. The absorption edge appeared at longer wavelength (320 nm) as the oxygen gas mixture reached 6 vol%. However, with an introduction oxygen gas in the sputtering process, the optical transmission significantly increased from around 95% (at 0% of O_2) to 99% (at 2% of O_2). The slight change was observed with further increase of the oxygen gas (around 99% T at 2% to 6% of O_2). The discussion for that will be later in this work.
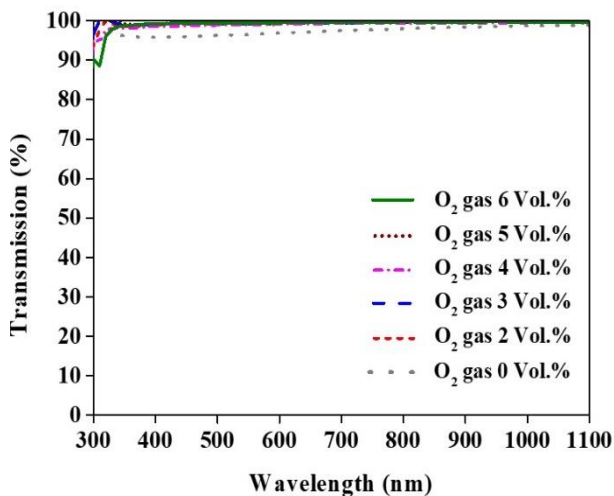

**Figure 3.** Influence of oxygen gas mixtures on optical transmission of the Al_2O_3 thin films.

3.2 Film structure and surface morphology

The X-ray diffraction profiles of the Al_2O_3 thin films deposited on glass substrate at room temperature with different oxygen gas mixtures were plotted in Figure 4. The XRD pattern showed an amorphous structure with no distinct diffraction peak but a hump centered at 2 Theta ~ 23° from the glass substrate (soda-lime-silica glass) [41]. Corresponding with works by García-Valenzuela et al. [9], the Al_2O_3 films deposited at room temperature were transparent with amorphous structure.

Effects of the oxygen gas mixtures on the surface morphology of the as-deposited Al_2O_3 thin films on silicon wafer substrate were investigated by FESEM. As seen in Figure 5, granular structure was observed in all the films especially with the sputtering condition at 0% of O_2.
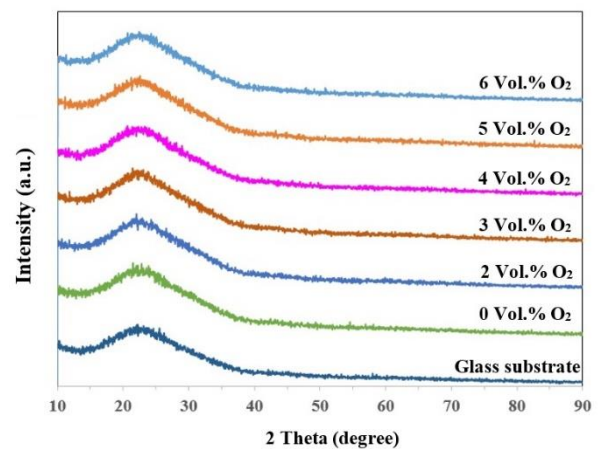
Figure 4. XRD diffraction patterns of the Al_2O_3 thin films with different vol% of O_2.
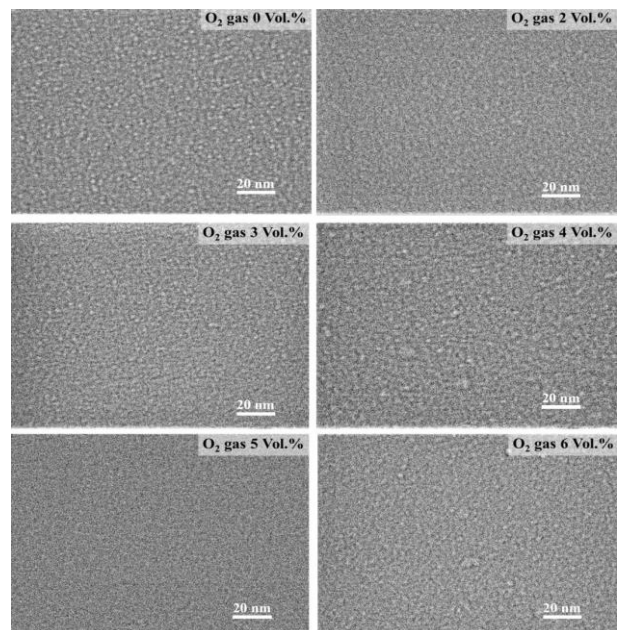
Figure 5. SEM image of the Al_2O_3 thin films deposited at different oxygen gas mixtures.

This surface structure is typical for thin films deposited by sputtering process [29-31]. A study by Tang *et al.*, 2019 [30] showed that the sputtered superfine Al_2O_3 particles were deposited onto a substrate during deposition process at room temperature. The particles arriving on the substrate possessed low kinetic energy with a short diffusion distance on the surface to form islands. The deposited Al_2O_3 islands with different sizes grew larger until they connected to create layer of the film. As being reported in research study of the thin film deposition from metal oxide targets by RF magnetron sputtering process, surface roughness of the thin films decreases significantly with a variation of oxygen gas partial pressure in the sputtering process [41-43].
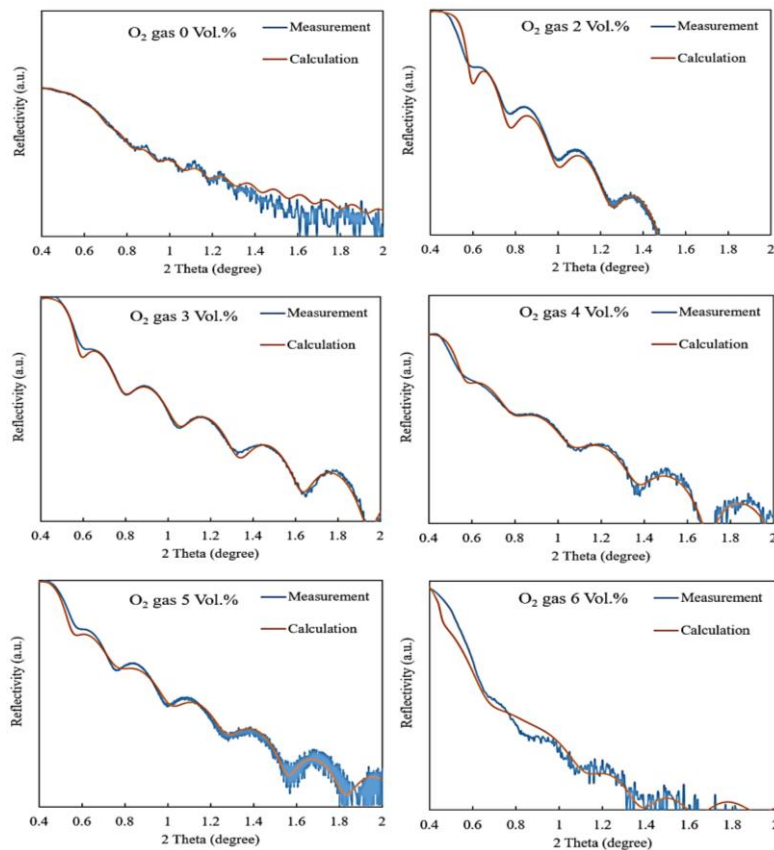
3.3 Chemical compositions and film thicknesses

Chemical compositions of the Al_2O_3 thin films coated on the stainless steel substrate by the RF magnetron sputtering were analyzed by XRF measurement which is a non-destructive method for elemental analysis of a wide range of materials including thin films. The stainless steel plate was used instead of the microscope glass slide to avoid the signal of Al_2O_3 from the soda-lime-silica glass substrate (about 0% to 3% Al_2O_3). According to the penetration depth of the X-ray, the different composition ratios of the substrate and thin film materials were detected depending on the thin layer on the substrate [43]. As tabulated in Table 1, the higher oxygen gas mixtures in the deposition process, the lesser percentages the Al_2O_3 thin film on the stainless steel substrate.

X-ray Reflectivity or XRR technique was also used to characterize thickness and density of the Al_2O_3 thin films deposited on silicon wafer substrate. The interference patterns of the reflected X-rays resulted from different Al_2O_3 thin film interfaces (Figure 6) varied with the oxygen gas mixtures. By fitting the different interference fringes, the thickness and density of the Al_2O_3 thin films were analyzed (Table 1). The variation of the film thickness as a function of the oxygen gas mixtures (Figure 7) corresponded with that of the percentage of the Al_2O_3 thin film on the substrate.

Table 1. Thickness, density and% of the Al_2O_3 films with different oxygen gas mixtures.

Oxygen gas (vol%)	Al_2O_3 thin film (wt%)	Thickness (nm)	Density (g·cm^{-3})
0	6.17	83.6	4.09
2	2.53	30.4	3.21
3	2.43	29.8	2.99
4	2.41	29.4	2.71
5	2.34	29.7	2.66
6	2.34	28.7	2.26

Figure 6. Reflectivity patterns of the Al_2O_3 thin films with various oxygen gas mixtures.
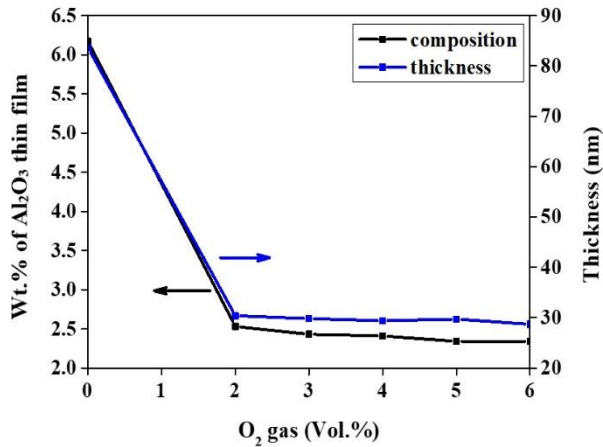
Figure 7. Influence of oxygen gas mixtures on thickness and percentage of the Al_2O_3 thin.
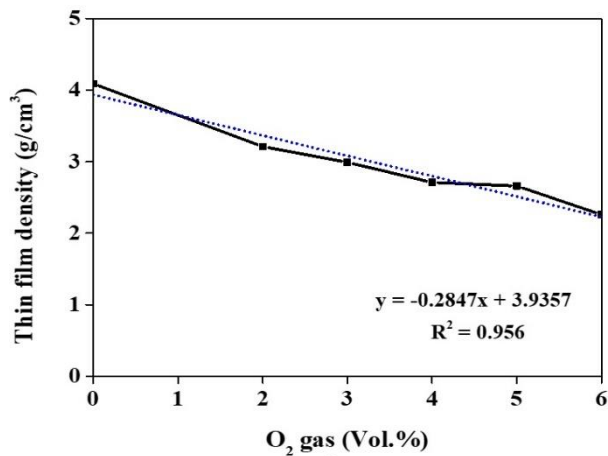
Figure 8. Influence of oxygen gas mixtures on density of the Al_2O_3 thin films.

The deposition process with 0 vol% of O_2 produced the Al_2O_3 thin film with maximum thickness (83.6 nm) corresponding with the maximum deposition rate (0.279 nm·min^{-1}). The more oxygen gas introduced in the sputtering system, the thinner the film thickness and the slower the deposition rate. With the variation of the oxygen mixtures, the thickness was reduced from 30.4 nm (at 2 vol% of O_2) to 28.7 nm (at 6 vol% of O_2). The deposition rates were reduced from 0.101 to 0.096 nm·min^{-1}, respectively. In good agreement with research works of Kim *et al.* [41] and Grayeli Korpi *et al.* [42], the film thickness decreases significantly with an introduction of oxygen gas in the sputtering process. The slight decrease of the film thickness with

further increase of the oxygen gas mixtures was explained by a slight reduction of the momentum transfer which reduced the sputtering yields of the sputtered particles (argon gas) to travel to the substrate. The reason for a significant decrease of the film thickness once the oxygen gas was introduced to the system is still unclear for the amorphous film. However, the same effect was observed on the crystalline thin film which was explained by the surface energy which plays a significant role on the orientation of the film [41].

In addition, with the variation of the oxygen gas mixture, density of the Al_2O_3 thin film was also decreased from 4.09 g·cm^{-3} (at 0 vol% of O_2) to 2.26 g·cm^{-3} (at 6 vol% of O_2) in linear trend with a slope of 0.28 (Figure 8). Obviously, the oxygen gas introduced in the system during the sputtering process interfered the sputtered alumina particles from travelling to the substrate and decelerated the deposition rate. Subsequently, the Al_2O_3 thin films grown in the oxygen-mixed sputtering ambient were lower in thickness, density and roughness in comparison with that in the argon gas only.

3.4 Scratch resistance

With the optimum 50 W of sputtering power and 6 vol% of oxygen gas mixture, the Al_2O_3 thin film was coated on semi-precious gemstones including peridot and aquamarine. An adhesion of the Al_2O_3 thin films on the gemstone was measured by microscratch tester with a maximum load of 20 N. The surface failure behavior of each sample was observed under a microscope on scratching with a progressive load along the scratch distance of 2 mm. Three different types of critical load (Lc) were indicated along the scratch trace; a start of the scratch (Lc1), delamination (Lc2) and complete delamination (Lc3) as shown in Table 2. Figure 9 and Figure 10 show the optical photographs of the scratch trace of the peridot and aquamarine, respectively, both (a) before and (b) after the Al_2O_3 thin film coating. Additionally, the scratch test values, such as the normal load (Fn) and the penetration depth (Pd) were also recorded along the scratch distance as seen in the optical photographs.

The results from scratch testing showed the complete delamination of the Al_2O_3 thin film coated on the gemstones. The critical loads on the peridot coated with the films were 10.0 N which was higher than that of stone without coating (8.8 N). The critical loads on the aquamarine before coating increased from 11.4 to 14.5 N after coating. The critical loads on the aquamarine were higher than those of the peridot since aquamarine has higher hardness [43]. The scratch resistance of two types of the semi-precious stones could be improve by coating with the Al_2O_3 thin films with the optimized coating condition by the RF magnetron sputtering technique.

Table 2. Scratch testing of the Al_2O_3 thin films grown on peridot and aquamarine.

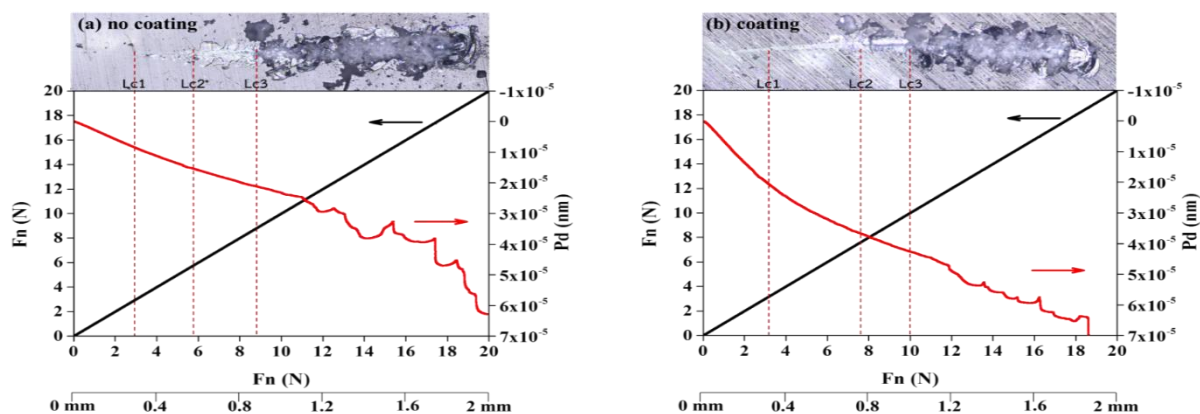| Semi-precious stone	Condition	Lc1 (N)	Lc2 (N)	Lc3 (N)
Peridot	No coating	2.90	5.83	8.77
	With coating	3.16	7.93	10.04
Aquamarine	No coating	5.96	8.35	11.43
	With coating	6.40	9.92	14.46

Figure 9. Scratch testing of peridot; (a) no coating; (b) coated with the Al$_2$O$_3$ thin films.

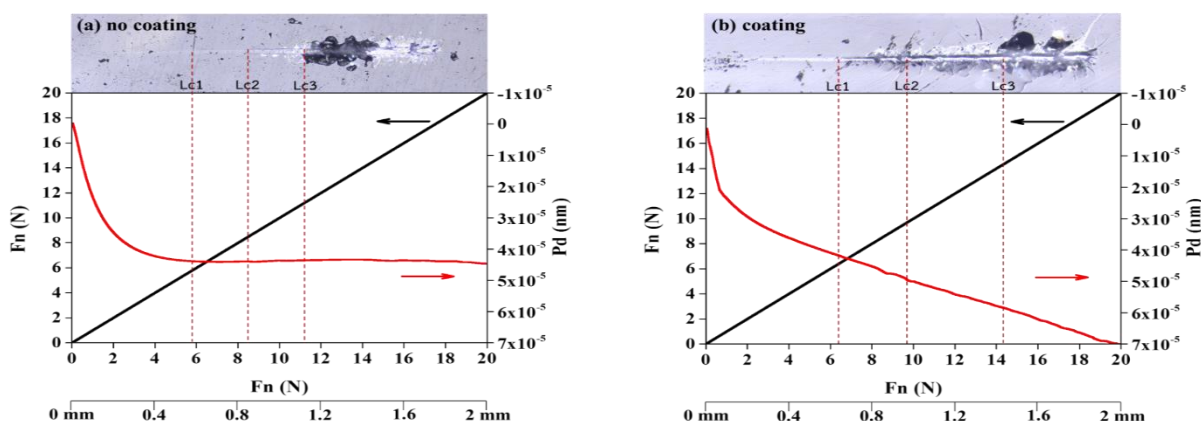**Figure 10.** Scratch testing of aquamarine; (a) no coating; (b) coated with the Al$_2$O$_3$ thin films.

4. Conclusions

Effects of RF sputtering power and oxygen gas mixtures on the Al$_2$O$_3$ thin films by the RF magnetron sputtering from the alumina target at room temperature were discovered. The deposition parameter was optimized from the investigation of optical property along with surface morphology and scratch resistance of the Al$_2$O$_3$ thin films. The optical transmission of the Al$_2$O$_3$ thin films was maximized around 95% to 99% at 50 W sputtering power and 6 vol% of O$_2$. All the films were amorphous phase with surface morphology in granular structure. Thickness of the Al$_2$O$_3$ thin films decrease significantly with an introduction of oxygen in the sputtering process from 83.6 nm (at 0% O$_2$) to 30.4 nm (at 2% O$_2$), and slowly decrease with an increase of the oxygen gas mixtures to 28.7 nm (at 6% O$_2$). Likewise, density of the Al$_2$O$_3$ thin films decrease linearly from 4.09 nm (at 0% O$_2$) to 2.26 nm. (at 2% O$_2$). The semi-precious gemstones (peridot and aquamarine) gained higher scratch resistance after the Al$_2$O$_3$ thin films coating. Their critical loads of peridot increased from 8.8 N (before coating) to 10.0 N (after coating). Similarly, for aquamarine, their critical loads increased from 11.4 N (before coating) to 14.5 N (after coating). The most optimum deposition condition for the Al$_2$O$_3$ thin film coating on the semi-precious gemstones to enhance the scratch resistance was determined to be 50 W of RF power, 6 vol% of O$_2$ mixture by the RF magnetron sputtering process at room temperature.

Acknowledgements

References

[1] I. Safi, "Recent aspects concerning DC reactive magnetron sputtering of thin films: A review," *Surface and Coatings Technology,* vol. 127, pp. 203-219, 2000.

[2] G. Zheng, X. Cheng, X. Yang, R. Xu, J. Zhao, and G. Zhao, "Self-organization wear characteristics of MTCVD-TiCN-Al$_2$O$_3$ coated tool against 300M steel," *Ceramics International*, vol. 43, pp. 13214-13223, 2017.

[3] N. Witit-Anun, and A. Buranawong, "Effect of sputtering power on the structure of DC magnetron sputtered vanadium nitride thin films," *Journal of Metals, Materials and Minerals*, vol. 27(1), pp. 47-52, 2017.

[4] P. Laha, A. B. Panda, S.K. Mahapatra, P. K. Barha, A. K. Das, and I. Banerjee, "Development of rf plasma sputtered Al₂O₃–TiO₂ multilayer broad band antireflecting coatings and its correlation with plasma parameters, *Applied Surface Science*, vol. 258, pp. 2275-2282, 2012.

[5] B. P. Dhonge, T. Mathews, S. T. Sundari, C. Thinaharan, M. Kamruddin, S. Dash, and A. K. Tyagi, "Spray pyrolytic deposition of transparent aluminum oxide (Al₂O₃) films," *Applied Surface Science*, vol. 258, pp. 1091-1096, 2011.

[6] J. Gottmann, and E. W. Kreutz, "Pulsed laser deposition of alumina and zirconia thin films on polymers and glass as optical and protective coatings," *Surface and Coatings Technology*, vol. 116-119, pp. 1189-1194, 1999.

[7] S. Prasanna, G. Mohan Rao, S. Jayakumar, M. D. Kannan, and V. Ganesan, "Dielectric properties of DC reactive magnetron sputtered Al₂O₃ thin films," *Thin Solid Films*, vol. 520, pp. 2689-2694, 2012.

[8] A. K. Hussain, and U-M. B. Al Naib, "Recent developments in graphene based metal matrix composite coatings for corrosion protection application: A review," *Journal of Metals, Materials and Minerals*, vol. 29(3), pp. 1-9, 2019.

[9] J. A. García-Valenzuela, R. Rivera, A. B. Morales-Vilches, L. G. Gerling, A. Caballero, J. M. Asensi, C. Voz, J. Bertomeu, and J. Andreu, "Main properties of Al₂O₃ thin films deposited by magnetron sputtering of an Al₂O₃ ceramic target at different radio-frequency power and argon pressure and their passivation effect on p-type c-Si wafers," *Thin Solid Films*, vol. 619, pp. 288-296, 2016.

[10] A. Wiatrowski, S. Patela, P. Kunicki, and W. Posadowski, "Effective reactive pulsed magnetron sputtering of aluminium oxide-properties of films deposited utilizing automated process stabilizer," *Vacuum*, vol. 134, pp. 54-62, 2016.

[11] P. Yaemsanguansak, M. Sittishoktram, R. Tuayjaroen, E. Ketsombun, T. Lertvanithphol, C. Luangchaisri, and T. Jutarosaga, "Modification of optical and structural properties of DC magnetron sputtered tungsten oxide thin films for electrochromic application," *Journal of Metals, Materials and Minerals*, vol. 29(2), pp. 79-86, 2019.

[12] D. C. Miller, R. R. Foster, S.-H. Jen, J. A. Bertrand, S. J. Cunningham, A. S. Morris, Y.-C. Lee, S. M. George, and M. L. Dunn, "Thermo-mechanical properties of alumina films created using the atomic layer deposition technique," *Sensors and Actuators A*, vol. 164, pp. 58-67, 2010.

[13] P. Boryło, K. Lukaszkowicz, M. Szindler, J. Kubacki, K. Balin, M. Basiaga, and J. Szewczenko, "Structure and properties of Al₂O₃ thin films deposited by ALD process," *Vacuum*, vol. 131, pp. 319-326, 2016.

[14] A. B. Khatibani, and S. M. Rozati, "Growth and molarity effects on properties of alumina thin films obtained by spray pyrolysis," *Materials Science in Semiconductor Processing*, vol. 18, pp. 80-87, 2014.

[15] S. Suchat, J. Potisart, S. Supprakob, G. Gitgeatpong, and P. Prachopchok, "Comparison of ZnO film prepared by spray pyrolysis and screen printing methods," *Journal of Metals, Materials and Minerals*, vol. 29(1), pp. 58-62, 2019.

[16] B. P. Dhonge, T. Mathews, N. Kumar, P. K. Ajikumar, I. Manna, S. Dash, and A. K. Tyagi, "Wear and oxidation resistance of combustion CVD grown alumina films," *Surface and Coatings Technology*, vol. 206, pp. 4574-4579, 2012.

[17] K. Wirandorn, N. Panyayao, and V. Siriwongrungson, "Characterization and photocatalytic activity of titanium dioxide deposited on stainless steel by pulsed-pressure MOCVD," *Journal of Metals, Materials and Minerals*, vol. 28(2), pp. 76-82, 2018.

[18] C. Breeding, A. Shen, S. Eaton-Magaña, G. Rossman, J. Shigley, and A. Gilbertson, "Developments in gemstone analysis techniques and instrumentation during the 2000s," *Gems & Gemology*, vol. 46(3), pp. 241-257, 2010.

[19] A. H. Shen, W. Wang, M. S. Hall, S. Novak, S. F. McClure, J. E. Shigley and T. M. Moses, "Serenity coated colored diamonds: Detection and durability," *Gems & Gemology*, vol. 43(1), pp.16-33, 2007.

[20] H. Gabasch, F. Klauser, E. Bertel, and T. Rauch, "Coloring of topaz by coating and diffusion processes: An X-ray photoemission study of what happens beneath the surface," *Gems & Gemology*, vol. 44(2), pp. 148-154, 2008.

[21] S. Eaton-Magaña, and K. M. Chadwick, "Cubic zirconia reportedly coated with nanocrystalline synthetic diamond", *Gems & Gemology*, vol. 45(1), pp.53-54, 2009.

[22] J. Shigley, A. Gilbertson, and S. Eaton-magaña, "Characterization of colorless coated cubic zirconia (diamantine)," *Gems & Gemology*, vol. 48(1), pp. 18-30, 2012.

[23] S. Tang, J. Su, T. Lu, Y. Ma, J. Ke, Z. Song, J. Zhang, and H. Liu, "A thick overgrowth of CVD synthetic diamond on a natural diamond," *The Journal of Gemmology*, vol. 36(2), pp. 134-141, 2018.

[24] S. Niyomsoan, C. Prapaipong, D. Boonyawan, and C. Umongno, "Synthesis and characterization of alumina thin film on semi-precious stones by plasma enhanced atomic layer deposition (PE-ALD)," *Proceeding of International Conference on Radiation and Emission in Materials (ICREM 2018),20-23 November 2018*, pp. 28-33, 2018, Chiang Mai, Thailand.

[25] C. Prapaipong, S. Niyomsoan, D. Boonyawan, and C. Umongno, "Alumina thin film synthesis for improving semi-precious stone quality with plasma enhanced atomic layer deposition (PE-ALD," *The 9ᵗʰ RMUTP International Conference on Science, Technology and Innovation for Sustainable Development: Challenges Towards the Digital Society, 21-22 June 2018*, pp. 42-55, The Sukosol, Thailand, 2018.

[26] S. Niyomsoan, C. Chomsaeng, S. Intarasiri, and D. Boonyawan, "Surface protective thin film on semi-precious gemstones by plasma-enhanced atomic layer (PE-ALD)," *Proceedings of Burapha University International Conference 2016, July 28-29*, pp. 305-312. Pattaya: Burapha University, 2016.

[27] G. Balakrishnan, R. Venkatesh Babu, K. S. Shin and J. I. Song, "Growth of highly oriented γ- and α-Al₂O₃ thin films by pulsed laser deposition," *Optics and Laser Technology*, vol. 56, pp. 317-321, 2014.

[28] M. M. Singh, H. Kumar, and P. Sivaiah, "Alumina thin film coatings at optimized conditions using RF magnetron sputtering process," *International Journal of Thin Films Science and Technology*, vol.10(1), pp13-20, 2021.

[29] G. Angarita, C. Palacio, M. Trujillo, and M. Arroyave, "Synthesis of alumina thin films using reactive magnetron sputtering method," *Journal of Physics: Conf. Series*, vol. 850, pp. 012022, 2017.

[30] X. Tang, Z. Li, H. Iiao, and J. Zhang, "Growth of ultrathin Al_2O_3 films on n-inp substrates as insulating layers by RF magnetron sputtering and study on the optical and dielectric properties," *Coatings*, vol. *9*, pp. 341, 2019.

[31] E. Turgut, Ö. Çoban, S. Sarıtaş, S. Tüzemen, M. Yıldırım, and E. Gür, "Oxygen partial pressure effects on the RF sputtered p-type NiO hydrogen gas sensors," *Applied Surface Science*, vol. 435, pp, 880-885, 2018.

[32] P. Mach, M. Kocián, and J. Kolářová, "Study of sputtering process of alumina thin films," *Proceedings of the 36th International Spring Seminar on Electronics Technology*, 8-12 May 2013, pp 247-252, 2013.

[33] E. Wallin, *Alumina Thin Films from Computer Calculations to Cutting Tools*. Linköping University, Sweden, 2008.

[34] M. Ahmadipour, S. N. Ayub, M. F. Ain, and Z. A. Ahmad, "Structural, surface morphology and optical properties of sputter-coated $CaCu_3Ti_4O_{12}$ thin film: Influence of RF magnetron sputtering power," *Materials Science in Semiconductor Processing*, vol. 66, pp. 157-161, 2017.

[35] Q. X. Guo, T. Tanaka, M. Nishio, and H. Ogawa, "Growth properties of AlN films on sapphire substrates by reactive sputtering," *Vacuum*, vol. 80(7), pp. 716-718, 2006.

[36] A. Iqbal, and F. Mohd-Yasin, "Reactive sputtering of aluminum nitride (002) thin films for piezoelectric applications: A review," *Sensors*, vol. 18, pp. 1797, 2018.

[37] B. Chapman, *Glow discharge processes: Sputtering and plasma etching*, 1st Edition, Kindle Edition, Wiley-interscience publication, John wiley & sons,1980.

[38] Y. Zhao, H. Wang, F. Yang, Z. Wang, J. Li, Y. Gao, Z. Feng, X. Li, and Z. Zhen, "Sputtering power induced physical property variation of nickel oxide films by radio frequency magnetron sputtering," *Mat. Res.,* vol. 21(2), pp. e20170836, 2018.

[39] C. H. Heo, S.-B. Lee, and J.-H. Boo, "Deposition of TiO_2 thin films using RF magnetron sputtering method and study of their surface characteristics," *Thin Solid Films*, vol. 475, pp. 183-188, 2005.

[40] R. Chakraborty, A. Dey, and A. K. Mukhopadhyay, "Loading rate effect on nanohardness of soda-lime-silica glass," *Metall Mater Trans A*, vol. 41, pp. 1301-1312, 2010.

[41] J-H Kim, J-H Lee, Y-W Heo, J-J Kim, and J-O Park, "Effects of oxygen partial pressure on the preferential orientation and surface morphology of ITO films grown by RF magnetron sputtering," *Journal of Electroceramics*, vol. 23, pp. 169-174, 2009.

[42] R. Grayeli Korpi, S. Rezaee, C. Luna, Ş. Ţălu, A. Arman, and A. Ahmadpourian, "Influence of the oxygen partial pressure on the growth and optical properties of RF-sputtered anatase TiO_2 thin films," *Results in Physics*, vol. 7, pp. 3349-3352, 2017.

[43] H. Fujiyama, T. Sumomogi, and T. Endo, "Effect of O_2 gas partial pressure on mechanical properties of SiO_2 films deposited by radio frequency magnetron sputtering," *Journal of Vacuum Science & Technology A*, vol. 20(2), pp. 356-361, 2002.